Sustainable Energy & Fuels

Particulate photocathode composed of (ZnSe)0.85(CuIn0.7Ga0.3Se2)0.15 synthesized with Na2S for enhanced sunlight-driven hydrogen evolution

Journal:	*Sustainable Energy & Fuels*
Manuscript ID	SE-ART-03-2018-000101.R1
Article Type:	Paper
Date Submitted by the Author:	11-Apr-2018

Complete List of Authors:	Kageshima, Yosuke; The University of Tokyo, Department of Chemical System Engineering Minegishi, Tsutomu; The University of Tokyo, Department of Chemical System Engineering; JST, PRESTO, Goto, Yosuke; The University of Tokyo, Department of Chemical System Engineering Kaneko, Hiroyuki; The University of Tokyo, Department of Chemical System Engineering Domen, Kazunari; The University of Tokyo, Department of Chemical System Engineering

Journal Name

ARTICLE

Particulate photocathode composed of $(ZnSe)_{0.85}(CuIn_{0.7}Ga_{0.3}Se_2)_{0.15}$ synthesized with Na_2S for enhanced sunlight-driven hydrogen evolution

Received 00th January 20xx,
Accepted 00th January 20xx

DOI: 10.1039/x0xx00000x

www.rsc.org/

Yosuke Kageshima,[a] Tsutomu Minegishi,[ab] Yosuke Goto, [‡ a] Hiroyuki Kaneko,[a] and Kazunari Domen*[a]

A particulate solid solution, $(ZnSe)_{0.85}(CuIn_{0.7}Ga_{0.3}Se_2)_{0.15}$, was synthesized by the flux method with using various amounts of a Cu precursor (to make Cu-deficient, stoichiometric, or Cu-excess specimens) and/or a Na_2S additive, to assess the effects of synthesis conditions on photoelectrochemical (PEC) properties. A stoichiometric $(ZnSe)_{0.85}(CuIn_{0.7}Ga_{0.3}Se_2)_{0.15}$ photocathode prepared with Na_2S produced a cathodic photocurrent in a neutral aqueous electrolyte approximately 2.3 times greater than that obtained from a sample made without Na_2S. Elemental analyses by inductively coupled plasma mass spectrometry and X-ray photoelectron spectroscopy demonstrated that the presence of Na_2S facilitated the incorporation of Li from the flux into the solid solution, in addition to the insertion of O atoms at Se vacancies, during the synthesis. Consequently, a $(ZnSe)_{0.85}(CuIn_{0.7}Ga_{0.3}Se_2)_{0.15}$ photocathode with appropriate surface modification and back contact demonstrated an onset potential for cathodic photocurrent as high as 0.77 V_{RHE}, a -5.2 mA cm^{-2} of photocurrent at 0 V_{RHE} and a half-cell solar-to-hydrogen conversion efficiency of 1.1% at 0.37 V_{RHE}. The present study provides new insights into techniques for the preparation of particulate Cu-chalcogenide photocathodes for efficient hydrogen evolution.

Introduction

Sunlight-driven water splitting to produce hydrogen and oxygen using semiconductor photocatalysts or photoelectrodes has attracted significant attention as a promising means of harvesting solar energy in the form of chemical energy.[1] Among the many possible photocatalytic materials, the group II-VI chalcogenides possess many attractive properties, such as long absorption edge wavelengths and band structures suitable for water splitting.[2] The majority of these chalcogenides exhibit n-type semiconducting properties, indicating that they would function as photoanodes.[3] However, these compounds are generally not stable under the conditions used to promote oxidation reactions.[4] Cu-chalcopyrites are among the most promising chalcogenides because they possess properties that allow them to act as photocathodes, including p-type semiconductivity, high optical absorption coefficients, usability in the polycrystalline state, high cathodic photocurrents at negative potentials, and stability during photoelectrochemical (PEC) reduction reactions.[5] Indeed, a polycrystalline $CuIn_{0.7}Ga_{0.3}Se_2$ (CIGS) photocathode has exhibited a half-cell solar-to-hydrogen (HC-STH) efficiency at 0.38 V versus a reversible hydrogen electrode (V_{RHE}) as high as 8.5%.[5c] Additionally, our own group has reported a polycrystalline (Cu,Ag)$GaSe_2$ photocathode capable of generating hydrogen from a weakly alkaline aqueous electrolyte under simulated sunlight in a stable manner for approximately 20 days.[5h]

Recently, we demonstrated novel polycrystalline thin-film photocathodes made from a solid solution of ZnSe and CIGS ($(ZnSe)_{0.85}(CIGS)_{0.15}$) that showed the beneficial features of both II-VI compounds and Cu-chalcopyrite, as noted above.[6] A $(ZnSe)_{0.85}(CIGS)_{0.15}$ photocathode prepared using a bilayer method exhibited a long absorption edge up to 900 nm and significant cathodic photocurrents as high as -12 and -4.9 mA cm^{-2} at 0 and 0.6 V_{RHE}, respectively, as well as a positive onset potential of approximately 0.9 V_{RHE} under simulated sunlight.[6b] As a consequence of the high cathodic photocurrent of the $(ZnSe)_{0.85}(CIGS)_{0.15}$ photocathode at positive potentials, a PEC cell consisting of this photocathode in conjunction with a $BiVO_4$ photoanode[7] successfully demonstrated overall water splitting with a solar-to-hydrogen (STH) conversion efficiency up to 1.0% without any external bias voltage.[8] The suitable onset potential of the $(ZnSe)_{0.85}(CIGS)_{0.15}$-based photocathode is attributed to a positive shift of the valence band maximum (VBM) relative to the shallow VBM of other CIGS-based material that result from the presence of Cu 3d orbitals.[5a, 9] It is probable that the VBM shift is triggered by the reduced Cu

[a] Department of Chemical System Engineering, The University of Tokyo, 7-3-1 Hongo, Bunkyo-ku, Tokyo 113-8656, Japan. E-mail: domen@chemsys.t.u-tokyo.ac.jp

[b] Japan Science and Technology Agency/Precursory Research for Embryonic Science and Technology (JST/PRESTO), 7-3-1 Hongo, Bunkyo-ku, Tokyo 113-8656, Japan.

† Electronic Supplementary Information (ESI) available: SEM images, XRD patterns, DR spectra and XPS data for various specimens, optimized sample preparation conditions, results of analysis of photoelectrochemical reaction products. See DOI: 10.1039/x0xx00000x

‡ Present address: Department of Physics, Tokyo Metropolitan University, Hachioji, Tokyo 192-0397 (Japan).

content in the former, resulting in a lesser contribution of Cu 3d orbitals to the formation of the valence band. In addition, we more recently reported that a $(ZnSe)_{0.85}(CIGS)_{0.15}$ photocathode can also be prepared from powdered materials (synthesized by a flux technique in a sealed quartz ampoule) via the particle transfer (PT) method.[10] The fabrication of photoelectrodes from powders has the potential to be economically feasible upon scale-up in the future, especially in comparison with polycrystalline units prepared under non-equilibrium conditions using vacuum co-evaporation. The possibility of fabricating integrated photoelectrodes on the microscopic scale, such as in the form of photocatalyst sheets, is another advantage of particulate photoelectrodes.[11] A particulate $(ZnSe)_{0.85}(CIGS)_{0.15}$ photocathode modified with sulphide layers composed of ZnS and CdS and a Pt catalyst generated a relatively large photocurrent of -4.3 mA cm^{-2} at 0 V_{RHE} and an onset potential of 0.8 V_{RHE} under simulated sunlight, even though it was prepared from powders.[10] In addition, a PEC cell fabricated from a particulate $(ZnSe)_{0.85}(CIGS)_{0.15}$-based photocathode and a $BiVO_4$ photoanode was found to be capable of driving overall water splitting under simulated sunlight with a 0.60% STH.[10]

In the past, both polycrystalline and particulate $(ZnSe)_{0.85}(CIGS)_{0.15}$ synthesized using an excess of Cu have been investigated as photocathodes.[6, 10] It is still unclear why an excess of Cu assists in producing active $(ZnSe)_{0.85}(CIGS)_{0.15}$ photocathodes, and the origin of the p-type semiconducting properties of this material is also unclear. Thus, additional information concerning the effects of the amount of Cu on the PEC properties of $(ZnSe)_{0.85}(CIGS)_{0.15}$ could be quite important to future material design research, as well as the development of more efficient photocathodes. In addition, it has been established that the introduction of alkali metal species enhances the photovoltaic performance of CIGS-based materials.[12] However, there have been no reports concerning the effects of alkali metal species on the PEC properties of Cu-chalcogenides. In the case of a previously reported polycrystalline thin-film $(ZnSe)_{0.85}(CIGS)_{0.15}$ photocathode prepared by the vacuum co-evaporation method, Na species could be incorporated from the soda-lime glass substrate, as has also been observed in conventional CIGS thin-film solar cells. Even so, Na doping into particulate $(ZnSe)_{0.85}(CIGS)_{0.15}$ has not yet been examined. This could represent one possible reason for the limited efficiencies of particulate $(ZnSe)_{0.85}(CIGS)_{0.15}$-based photocathodes compared to polycrystalline thin films, although the lack of detailed studies of synthesis conditions makes it difficult to draw conclusions.

In the present study, the synthesis conditions applied in the fabrication of $(ZnSe)_{0.85}(CIGS)_{0.15}$ particles were carefully investigated to examine the relationship between the particle composition and PEC performance. Particulate $(ZnSe)_{0.85}(CIGS)_{0.15}$ was initially synthesized by a flux method using various amounts of a Cu precursor (producing either Cu-deficient, stoichiometric, or Cu-excess materials), to clarify the effects of the amount of Cu on the p-type semiconducting properties and PEC performances of the resulting solid solution. In addition, Na doping into the $(ZnSe)_{0.85}(CIGS)_{0.15}$ particles was also examined, using Na_2S as the additive. These strategies were found to be effective at enhancing the PEC performances of the particulate photocathodes. As a result, this work provides new insights into the design of particulate Cu-chalcogenide photocathodes for efficient hydrogen evolution.

Experimental

Synthesis of $(ZnSe)_{0.85}(CIGS)_{0.15}$ particles

Particulate $(ZnSe)_{0.85}(CIGS)_{0.15}$ was synthesized by the flux technique in sealed quartz tubes according to a previously reported method.[10] The precursors, ZnSe, Cu_2Se, In_2Se_3, Ga_2Se_3 and Se powders, were purchased from the Kojundo Chemical Laboratory Co., Ltd., whereas LiCl, KCl and Na_2S were purchased from Wako Pure Chemical Industries. LiCl and KCl were dehydrated by heating at 200 °C for 1 h under vacuum prior to use. Prior to each synthesis, ZnSe and Ga_2Se_3 powders were ball-milled in ethanol to obtain fine particles, and then combined with Cu_2Se, In_2Se_3, Se, LiCl, KCl and Na_2S in a nitrogen-filled glovebox. The Zn/(Zn + In + Ga), Ga/(In + Ga) and LiCl/KCl molar ratios in the mixture were 0.85, 0.3 and 1.5, respectively. The amounts of the Cu precursor and Na_2S additive were varied to give Cu/(In + Ga) and Na/Cu molar ratios in the ranges of 0.9—1.4 and 0—1, respectively. It should be noted that the optimal molar ratio for the Na_2S additive was Na/Cu = 0.2, as discussed in the Electronic Supplementary Information (ESI). Each mixture was subsequently sealed in a quartz ampoule and heated at 500 °C for 15 h. The calcination duration was separately optimized, as described in the ESI. Following this heat treatment, the resulting $(ZnSe)_{0.85}(CIGS)_{0.15}$ particles were separated from the chloride flux by several washes with distilled water. The $(ZnSe)_{0.85}(CIGS)_{0.15}$ particles synthesized at Cu/(In + Ga) ratios < 1, 1 and > 1 are denoted herein as Cu-deficient, stoichiometric, and Cu-excess specimens.

Fabrication of the particulate photocathodes

Photocathodes made of the particulate $(ZnSe)_{0.85}(CIGS)_{0.15}$ were subsequently fabricated using the PT method.[10, 13] The synthesized particles were coated onto a clean glass substrate by drop casting a suspension of the photocatalyst powder in isopropanol, followed by drying. A Mo and/or C contact layer and a Ti conductor layer were then deposited in sequence on the photocatalyst layer by radio frequency (RF)-magnetron sputtering. During the deposition of contact and conductor layer, temperature of the glass substrate was kept at 200 °C. It should be noted that a thin Mo and subsequent C and Ti layers were deposited on the particles in the case of a Mo and C bilayer, denoted Mo/C. The details regarding the optimization of contact layer thickness are provided in the ESI. The final assembly, consisting of the metal layers and $(ZnSe)_{0.85}(CIGS)_{0.15}$ particles, functioned as a photocathode after fixing the layers on a second glass plate using carbon tape and removing excessive particles by sonication.

Prior to the following surface modifications, the electrode surface was etched with an aqueous solution containing 0.1 M KCN and 0.8 M KOH for 1 min, followed by rinsing with distilled water. The photocathode was then modified with a CdS and/or ZnS layer via chemical bath deposition (CBD), employing a previously reported procedure.[10] CBD was performed with 50 mL of an aqueous solution containing 25 mM $Cd(CH_3COO)_2$, 0.375 M $SC(NH_2)_2$ and 14 wt% ammonia as precursors. During the deposition period of 14 min, the beaker containing the precursors and photocathode was immersed in a water bath held at 60 °C, resulting in a gradual increase in the temperature of the reaction mixture to approximately 53 °C. The ZnS layer was then applied in the same manner but using $Zn(CH_3COO)_2$ as the precursor instead of $Cd(CH_3COO)_2$. Following these CBD processes, each specimen was annealed at 200 °C for 1 h in air. A Pt catalyst for the hydrogen evolution reaction was subsequently deposited on the photocathode by photo-electrodeposition using a three-electrode system in an aqueous electrolyte containing 10 μM H_2PtCl_6, 100 μM NaOH and 0.1 M Na_2SO_4. A solar simulator generating AM 1.5G radiation at 100 $mWcm^{-2}$ was used as a light source. During the photo-electrodeposition of Pt particles, a constant potential of −0.3 V versus Ag/AgCl ($V_{Ag/AgCl}$) was applied to the photocathode. It should be noted that irradiation with simulated sunlight was maintained until the photocurrent plateaued (approximately 1 h). The photocathodes produced in this manner are hereafter referred to as Pt/(ZnS/)CdS/$(ZnSe)_{0.85}(CIGS)_{0.15}$/*M*/Ti (*M* = Mo, C or Mo/C).

Characterization of $(ZnSe)_{0.85}(CIGS)_{0.15}$ particles

Structural analyses of the prepared powders and electrodes were conducted using scanning electron microscopy (SEM; Hitachi, S-4700). The elemental compositions of the powders were analysed by inductively coupled plasma mass spectrometry (ICP-MS; Agilent, 7700) in dilute nitric acid, and by X-ray photoelectron spectroscopy (XPS; JEOL, JPS-9000) with the Mg Kα line. The XPS analyses were conducted using a particulate $(ZnSe)_{0.85}(CIGS)_{0.15}$/Mo/Ti photocathode whose surface had been etched by Ar ion sputtering. The details of the XPS analyses and the Cu, O, and Se depth profiles from the surfaces of the electrodes are also provided in the ESI. The crystalline properties of the synthesized powders were characterized by X-ray diffraction (XRD; Rigaku, RINT Ultima III) using the Cu Kα line. The optical properties and absorption edges of the particles were assessed by UV-visible diffuse reflectance spectroscopy (UV-vis DRS; Jasco, V-670).

Photoelectrochemical measurements

The PEC measurements were conducted in a typical three-electrode setup. A Pt wire and Ag/AgCl in saturated KCl were used as the counter and reference electrodes, respectively. A 1.0 M potassium phosphate solution (KPi; KH_2PO_4/K_2HPO_4 = 50/50, adjusted to pH 7.0 using aqueous KOH) purged with Ar was used as the electrolyte. This was vigorously stirred to ensure homogeneity during all PEC measurements. Samples were irradiated with simulated sunlight adjusted to AM 1.5G.

Results and discussion

Effects of the amount of Cu on the physical and photoelectrochemical properties

All diffraction peaks in the XRD patterns of the specimens prepared with various amounts of the Cu precursor (Fig. 1a) can be assigned to a zincblende phase, indicating the successful formation of a solid solution of ZnSe (having a zincblende structure) and CIGS (having a chalcopyrite structure), similar to the results of previous studies.[6, 10] The samples all showed similar degrees of crystallinity regardless of the Cu loading. The stoichiometric and 20—40% Cu-excess $(ZnSe)_{0.85}(CIGS)_{0.15}$ particles had absorption edges at approximately 800 nm, while the absorption edge of the Cu-deficient solid solutions were slightly blue-shifted to 700—750 nm, as shown in the DRS data in Fig. 1b, similar to results previously obtained for CIGS.[14] The minimal amount of light absorption at longer wavelengths (above 800 nm) in the case of the Cu-excess samples was continuously reduced as the Cu

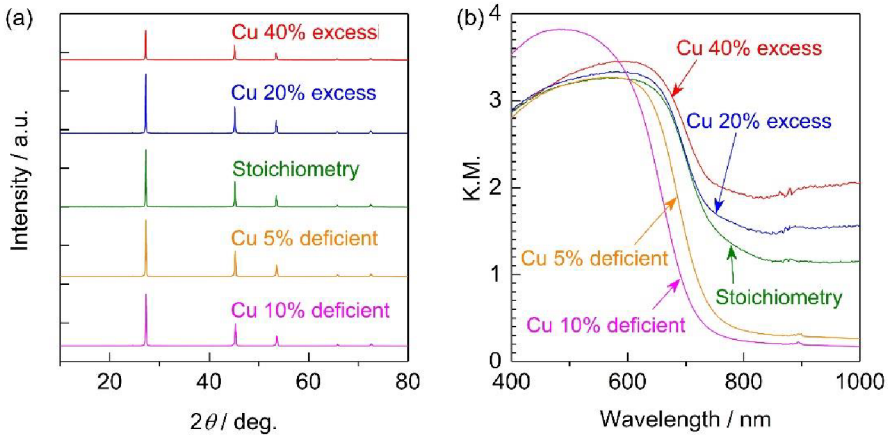

Fig. 1 (a) XRD patterns and (b) DR spectra for 20—40% Cu-excess, stoichiometric, and 5—10% Cu-deficient $(ZnSe)_{0.85}(CIGS)_{0.15}$ particles synthesized by the flux method.

loading approached the stoichiometric value. Moreover, the 5—10% Cu-deficient materials exhibited clearly reduced absorption in the longer wavelength region relative to the estimated absorption edge compared to the Cu-excess material. It has been reported that the optical absorption of CIGS at low energies increases as the Cu content increases,[15] and that weak absorption at wavelengths longer than the absorption edge suggests the presence of defects or impurity phases.[16] Based on the DRS results, using either stoichiometric or deficient Cu amounts appears to be favourable from the viewpoint of the optical properties. The morphology of $(ZnSe)_{0.85}(CIGS)_{0.15}$ particles clearly changed according to the amount of Cu precursor, as can be seen in the SEM images (Fig. 2). It was observed that the stoichiometric and Cu-excess $(ZnSe)_{0.85}(CIGS)_{0.15}$ particles had a rugged, poorly-defined morphology with a wide range of particle sizes, from submicron to several micron, which is consistent with previous findings.[10] In contrast, the Cu-deficient $(ZnSe)_{0.85}(CIGS)_{0.15}$ particles showed triangular features with submicron sizes, indicating that a reduced Cu loading appears to assist in generating clear crystalline facets.

The PEC performances of particulate photocathodes consisting of $(ZnSe)_{0.85}(CIGS)_{0.15}$ synthesized with various amounts of the Cu precursor and having the structure of $Pt/CdS/(ZnSe)_{0.85}(CIGS)_{0.15}/Mo/Ti$ were evaluated in a neutral buffer solution under simulated sunlight (Fig. 3). Each solid solution showed an obvious cathodic photoresponse at negative potentials, even in the case of the Cu-deficient material. The $(ZnSe)_{0.85}(CIGS)_{0.15}$ synthesized with a 40% Cu excess (equivalent to the conventional approach) exhibited the best PEC performance, with a 0.65 V_{RHE} onset potential and a -2.4 mA cm^{-2} photocurrent at 0 V_{RHE}. In contrast, the photocurrents generated by the photocathodes prepared using a reduced amount of Cu gradually deteriorated compared to the above values as the Cu loading was decreased. In particular, the Cu-deficient samples produced very low cathodic photocurrents at negative potentials in conjunction with an obvious anodic photoresponse at positive potentials (Fig. 3b). These results were obtained despite the favourable optical properties and clear crystalline facets of the Cu-deficient materials. It is well-known that conventional CIGS-based materials synthesized using Cu-deficient condition typically exhibit superior photovoltaic or PEC performances,

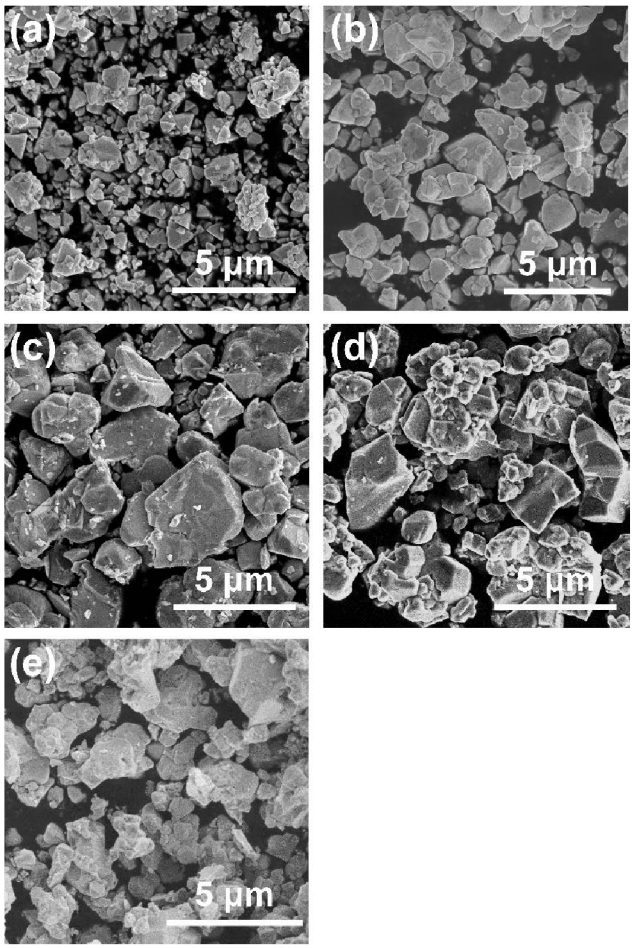

Fig. 2 SEM images of (a) 10% Cu-deficient, (b) 5% Cu-deficient, (c) stoichiometric, (d) 20% Cu-excess, and (e) 40% Cu-excess $(ZnSe)_{0.85}(CIGS)_{0.15}$ particles. Scale: 5 μm.

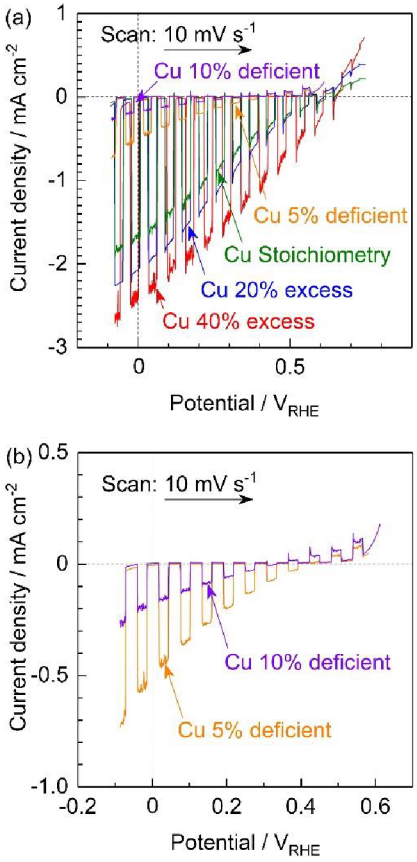

Fig. 3 (a) Current-potential curves for $Pt/CdS/(ZnSe)_{0.85}(CIGS)_{0.15}/Mo/Ti$ photocathodes prepared by the PT method. The photocatalyst particles were synthesized using various amounts of the Cu precursor to produce 20—40% Cu-excess, stoichiometricm, and 5—10% Cu-deficient particles. The current-potential curves for the Cu-deficient $(ZnSe)_{0.85}(CIGS)_{0.15}$ photocathodes are enlarged in (b). Electrolyte: 1 M KPi (pH = 7). Light source: simulated sunlight (AM 1.5G).

because their p-type semiconducting properties originate from Cu vacancies.[12b] The anodic photoresponse observed in the present study implies that these materials possessed n-type semiconducting properties to a certain extent. In this research, the Zn^{2+} ions substituted at Cu^{+} sites would be expected to function as donors. However, an excess of the Cu precursor in the conventional synthesis method would prevent the formation of Zn_{Cu} anti-sites, resulting in active photocathodes. In addition, the smaller particle sizes of the Cu-deficient solid solutions could also be considered as one possible cause for the reduced PEC performances.

Improvements in the photoelectrochemical performances by using the Na_2S additive

Since it was determined that the Cu-excess and stoichiometric $(ZnSe)_{0.85}(CIGS)_{0.15}$ were capable of generating significant cathodic photocurrents and no obvious anodic photoresponses, Na doping via the addition of Na_2S was applied to the stoichiometric and 40% Cu-excess particles. The DR spectra obtained from the $(ZnSe)_{0.85}(CIGS)_{0.15}$ particles synthesized with and without Na_2S are compiled in Fig. 4. All solid solutions exhibited an absorption edge in the vicinity of 800 nm together with weak light absorption at longer wavelengths. It should be noted that the absorption of the stoichiometric $(ZnSe)_{0.85}(CIGS)_{0.15}$ above 800 nm was reduced compared with that of the Cu-excess specimen, regardless of the use of Na_2S. These results demonstrate that stoichiometric $(ZnSe)_{0.85}(CIGS)_{0.15}$ particles synthesized with Na_2S possess favourable optical properties, such that further enhancement of the PEC properties can also be expected. The morphology of the particles was also clearly changed upon using the Na_2S (Fig. 5). It was observed that both the stoichiometric and 40% Cu-excess $(ZnSe)_{0.85}(CIGS)_{0.15}$ synthesized with Na_2S were composed of triangular crystal with relatively large sizes on the order of microns, in contrast to the particles synthesized without Na_2S (Fig. 2).

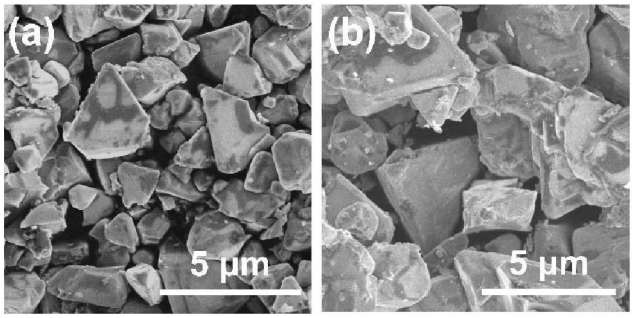

Fig. 5 SEM images of (a) stoichiometric and (b) 40% Cu-excess $(ZnSe)_{0.85}(CIGS)_{0.15}$ particles synthesized with Na_2S. Scale: 5 μm.

The Na_2S significantly improved the cathodic photocurrent but did not affect the onset potential, as can be seen in the current-potential curves in Fig. 6. The cathodic photocurrent generated by the 40% Cu-excess $(ZnSe)_{0.85}(CIGS)_{0.15}$ photocathode was enhanced by a factor of approximately 1.8 by Na_2S addition (from -2.4 to -4.2 mA cm^{-2} at 0 V_{RHE}), while that of the stoichiometric $(ZnSe)_{0.85}(CIGS)_{0.15}$ photocathode was increased by a factor of 2.3 (from -1.7 to -3.9 mA cm^{-2} at 0 V_{RHE}). The relatively large particles with clear crystal facets in the SEM images (Fig. 5) are consistent with the significantly enhanced PEC performances of the $(ZnSe)_{0.85}(CIGS)_{0.15}$ samples synthesized with Na_2S. As described in the ESI, with increases in the amount of Na_2S, the cathodic photocurrent was initially drastically improved but then gradually decreased with further increases in the quantity of the additive. As a result, the highest photocurrent was obtained at a Na/Cu (or Na/(In + Ga)) ratio of 0.2. It is particularly important that, although the photocurrent generated by the stoichiometric $(ZnSe)_{0.85}(CIGS)_{0.15}$ photocathode was approximately 30% lower than that produced by the 40% Cu-excess specimen when each was made without Na_2S, both the stoichiometric and Cu-excess $(ZnSe)_{0.85}(CIGS)_{0.15}$ synthesized with Na_2S

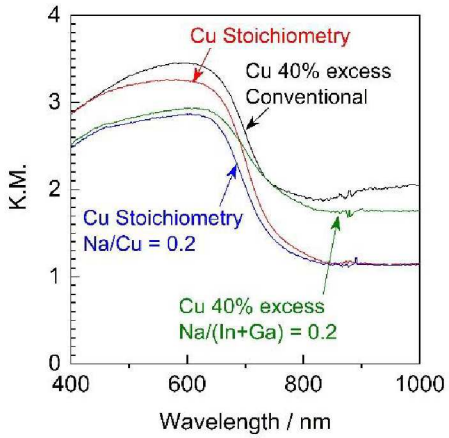

Fig. 4 DR spectra acquired from stoichiometric or 40% Cu-excess $(ZnSe)_{0.85}(CIGS)_{0.15}$ particles synthesized with and without Na_2S at Na/Cu (or Na/(In + Ga)) = 0.2.

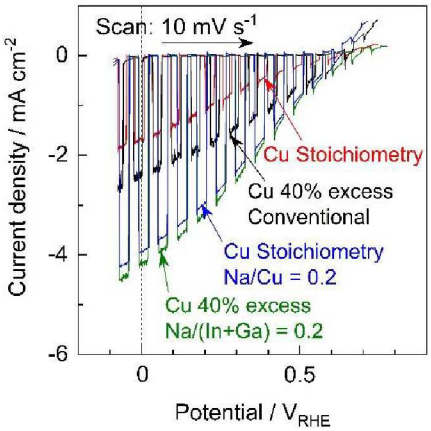

Fig. 6 Current-potential curves for Pt/CdS/$(ZnSe)_{0.85}(CIGS)_{0.15}$/Mo/Ti photocathodes consisting of $(ZnSe)_{0.85}(CIGS)_{0.15}$ particles synthesized under stoichiometric or 40% Cu-excess conditions with and without Na_2S via the PT method. Electrolyte: 1 M KPi (pH = 7). Light source: simulated sunlight (AM 1.5G).

showed similar photocurrents (up to approximately -4 mA cm^{-2} at 0 V_{RHE}). Therefore, it can be concluded that the use of Na_2S improved the cathodic photocurrent either with an excess or a stoichiometric amount of Cu, despite the coexistence of Zn species, which is capable of acting as donors.

To reveal the effects of stoichiometry of precursor and of adding Na_2S to the precursor onto the elemental composition of the $(ZnSe)_{0.85}(CIGS)_{0.15}$ particles, ICP-MS analysis was conducted. As shown in Fig. 7a, amount of Cu in the resulting samples increased with the amount of Cu species in precursors at stoichiometric and Cu-excessive synthesis conditions. The Cu-deficient synthesis conditions resulted in increases in the amounts of Zn and Li. This occurred as a result of the formation of Zn_{Cu} anti-sites and Li_{Cu}. As noted above, Zn_{Cu} anti-sites can act as donors. However, the $(ZnSe)_{0.85}(CIGS)_{0.15}$ functioned as a photocathode material, suggesting that the Li_{Zn} in this solid solution could work as acceptors that compensate for the presence of donors. The radii of the Zn^{2+}, Cu^{+} and Li^{+} ions are 74, 74 and 73 pm, respectively, so these ions readily substitute for one another.[17] The Li concentration in the solid solution reached to 0.18% at a Cu/(In+Ga) ratio of 0.9. In contrast, K^{+} has a much larger ionic radius of 151 pm, so that the extent of K substitution was negligible.[17] The compositions of samples synthesized with stoichiometric amounts of the precursors and differing quantities of Na_2S are summarized in Fig. 7b. In keeping with the data in Fig. 7a, Na was not detected in these materials despite the use of Na_2S, possibly due to its large ionic radius (113 pm) in a four-coordinated state.[17] Instead, the Na_2S greatly facilitated the incorporation of Li, while the levels of Zn, Cu, In and Ga were almost constant. Using a very large quantity of Na_2S (Na/Cu = 1), approximately 5.3% Li was incorporated into the solid solution and the Zn content was decreased from approximately 72.1% (with no Na_2S addition) to 67.8%, while the Cu content slightly decreased, from 12.8% to 11.9%. These results imply that a large proportion of the Li was introduced at the Zn sites. Although the details of the local structures are still unclear, Li ions at Zn sites could function as acceptors, whereas Li ions at Cu sites would be expected to prevent the formation of Zn anti-sites.

In addition, XPS analyses determined that the O/Se ratio in the photocatalyst particles gradually increased according to the amount of Na_2S addition, while the Se/Cu ratio remained constant (Fig. 8). It should be noted that these elemental ratios are based on the peak areas in XPS spectra. This was done because the surfaces of the present particulate photocathodes possessed micron-ordered roughness, whereas the escape depth of photoelectrons is on the order of nm, such that quantitative evaluations of the actual elemental compositions in the overall bulk particles is difficult. It has been reported that Na species exhibit catalytic effects for the surface oxidation of semiconductors, related to the passivation of Se vacancies in the CIGS.[18] The present XPS observations imply that the Na_2S might promote the insertion of O atoms into Se vacancies during the growth of the material. In addition, it is

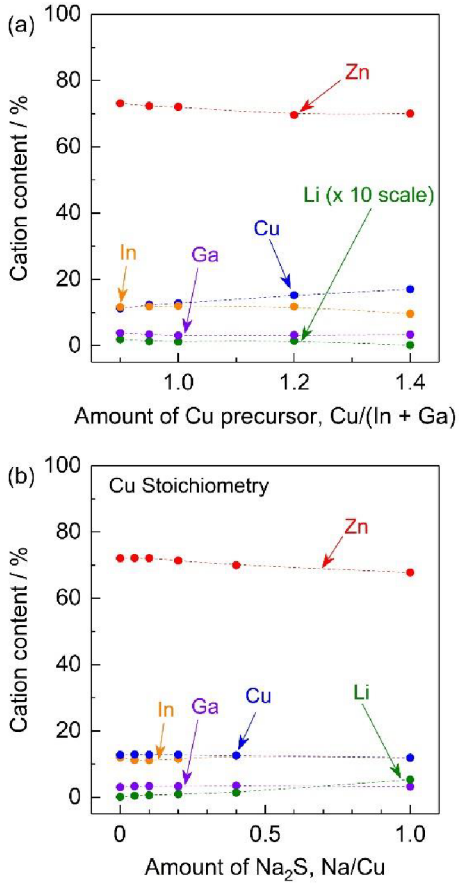

Fig. 7 Levels of Zn, Cu, In, Ga and Li in (a) $(ZnSe)_{0.85}(CIGS)_{0.15}$ particles synthesized with various amounts of Cu precursor, Cu/(In + Ga) = 0.9—1.4, without Na_2S, and (b) stoichiometric $(ZnSe)_{0.85}(CIGS)_{0.15}$ synthesized with various amounts of Na_2S Na/Cu = 0—1. The term cation content indicates M/(Zn + Cu + In + Ga + Li), M = Zn, Cu, In, Ga or Li.

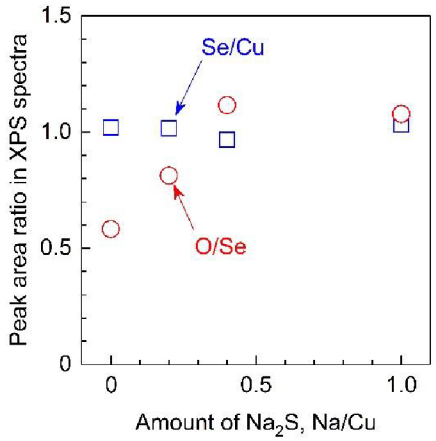

Fig. 8 Ratios of Se/Cu and O/Se peak areas in XPS spectra for stoichiometric $(ZnSe)_{0.85}(CIGS)_{0.15}$ particles as a function of the relative amount of Na_2S used. The XPS data were acquired from $(ZnSe)_{0.85}(CIGS)_{0.15}$ photocathodes prepared by a PT method and surface etched with an ion beam to remove the oxidized surface.

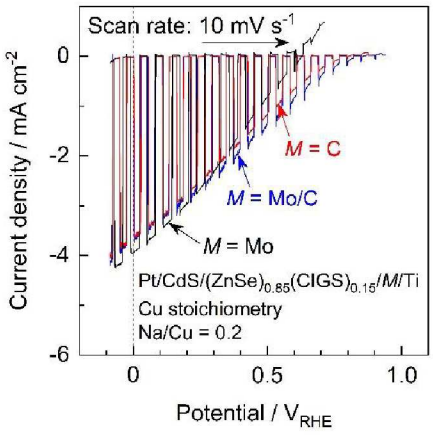

Fig. 9 Current-potential curves for Pt/CdS/$(ZnSe)_{0.85}(CIGS)_{0.15}$/*M*/Ti photocathodes prepared by the PT method with various contact layers: M = Mo, C or Mo/Ti. $(ZnSe)_{0.85}(CIGS)_{0.15}$ particles were synthesized under stoichiometric conditions with Na_2S. Electrolyte: 1 M KPi (pH = 7). Light source: simulated sunlight (AM 1.5G).

also possible that the Li incorporated into the particulate solid solutions by the use of the Na_2S may have similar effects to Na species with regard to promoting oxidation.[18] Considering the ICP-MS and XPS data, it is evident that the Na_2S increases the incorporation of Li from the flux into the solid solution, accompanied by the introduction of O atoms at Se vacancies.

Effect of the electrode structure on the photoelectrochemical properties of the photocathodes

The present $(ZnSe)_{0.85}(CIGS)_{0.15}$ photocathode prepared by the PT method generated a relatively large anodic dark current at positive potentials above 0.7 V_{RHE}, which is attributed to either the oxidation of Mo or the $MoSe_2$ backside contact layer (Figs. 3 and 6).[10] This large current can negatively shift the onset potential for the cathodic photocurrent. Since a positive onset potential for the photocathode is indispensable to the efficient functioning of a PEC cell using an appropriate photoanode to drive overall water splitting without any external bias voltage, suppression of the anodic dark current is important. Previously, we found that using C rather than Mo as the contact eliminated the dark current derived from oxidation of Mo species and improved the onset potential of a particulate $(ZnSe)_{0.85}(CIGS)_{0.15}$ photocathode prepared by the PT method.[10] However, in this same prior work, a photocathode with a C contact layer generated a higher photocurrent at positive potentials but a lower photocurrent in the vicinity of 0 V_{RHE} compared to a photocathode with a Mo contact layer. Hence, we examined the effects of the back contact material on both the onset potential and cathodic photocurrent of the present particulate $(ZnSe)_{0.85}(CIGS)_{0.15}$ photocathode.

Current-potential curves obtained from a particulate photocathode with various back contacts, Pt/CdS/$(ZnSe)_{0.85}(CIGS)_{0.15}$/*M*/Ti: *M* = Mo, C, and with a Mo/C bilayer, are presented in Fig. 9. The stoichiometric $(ZnSe)_{0.85}(CIGS)_{0.15}$ synthesized with Na_2S was employed in these trials. As a result of a detailed optimization of the thickness of the C contact layer (see ESI), a particulate $(ZnSe)_{0.85}(CIGS)_{0.15}$ photocathode with a nominally 6.5 nm thick C contact layer exhibited a positive onset potential as high as 0.8 V_{RHE} as well as a photocurrent comparable to that obtained with a Mo back contact (-3.6 mA cm^{-2} at 0 V_{RHE}). The C layer formed by sputtering deposition was quite fragile, and an overly thick C contact layer resulted in a loss of photocatalytic particles or interruption of the in-plane electrical conductivity. In contrast, in the case of an overly thin C contact layer, $(ZnSe)_{0.85}(CIGS)_{0.15}$ particles were in partial contact with the Ti conductor layer, thus forming a partial Shottky contact and supressing the photocurrent, as discussed in the ESI. Thus, an appropriate C layer thickness must balance an enhanced onset potential and photocurrent. In order to further improve the cathodic photocurrent, a thin (nominally 15 nm) Mo layer was

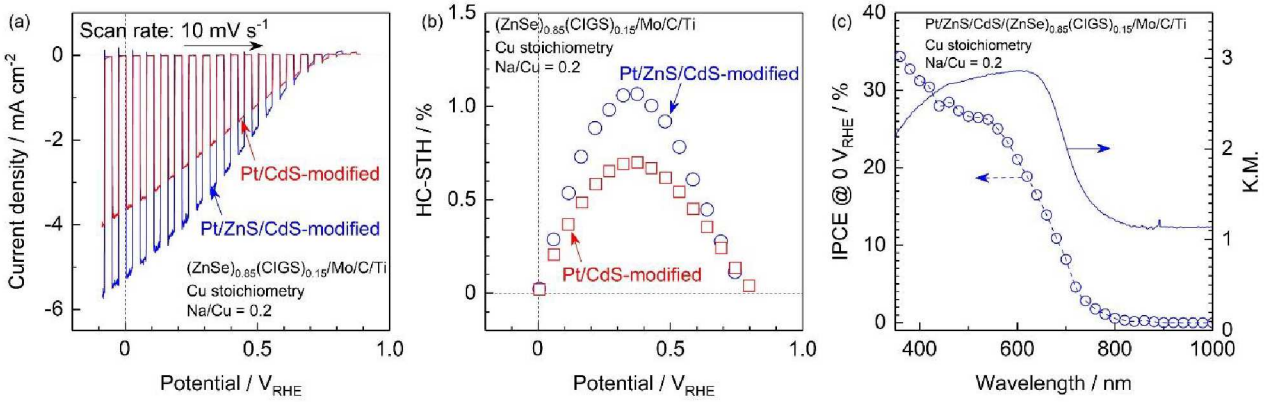

Fig. 10 (a) Current-potential curves, (b) half-cell solar-to-hydrogen conversion efficiency (HC-STH) values, and (c) the incident-photon-to-current conversion efficiency (IPCE) spectrum of Pt/ZnS/CdS/$(ZnSe)_{0.85}(CIGS)_{0.15}$/Mo/C/Ti photocathodes. $(ZnSe)_{0.85}(CIGS)_{0.15}$ particles were synthesized under stoichiometric conditions with Na_2S. PEC data for a $(ZnSe)_{0.85}(CIGS)_{0.15}$ photocathode modified with only a Pt/CdS layer are also compiled in (a) and (b). The DR spectrum of the photocatalyst particles is provided in (c). Electrolyte: 1 M KPi (pH = 7). Light source: simulated sunlight (AM 1.5G) for (a) and (b), and 300 W Xe lamp equipped with a monochromator for (c).

inserted between the $(ZnSe)_{0.85}(CIGS)_{0.15}$ particles and the C contact layer. The particulate $(ZnSe)_{0.85}(CIGS)_{0.15}$ photocathode with a Mo/C bilayer contact showed similar and slightly larger cathodic photocurrents at 0 V_{RHE} and at positive potentials, respectively, compared to the samples with solely Mo or C monolayer contacts. Remarkably, a Pt/CdS/$(ZnSe)_{0.85}(CIGS)_{0.15}$/Mo/C/Ti photocathode exhibited the highest cathodic photocurrent over the potential range of 0.3—0.85 V_{RHE} among the examined photocathodes. We suggest that the incorporation of a small amount of Mo between the $(ZnSe)_{0.85}(CIGS)_{0.15}$ particles and the C contact layer leads to superior Ohmic contact at the semiconductor-contact layer interface.[19]

It has also been reported that sulphide overlayers composed of ZnS and CdS further enhance the cathodic photocurrent due to the increased thickness of the depletion layer at the solid–liquid interface and the promotion of charge separation.[10] Thus, surface modification with a ZnS/CdS bilayer was also applied to the present particulate photocathode made from stoichiometric $(ZnSe)_{0.85}(CIGS)_{0.15}$ synthesized with Na_2S. The Pt and ZnS/CdS-modified photocathode generated a far higher cathodic photocurrent than a Pt/CdS-modified specimen, with a value as high as -5.2 mA cm^{-2} at 0 $V_{RHE.}$ The onset potential also remained comparable to that of a Pt/CdS-modified cathode (Fig. 10a). The faradaic efficiency during PEC hydrogen evolution was confirmed to be almost 100% based on analyses via gas chromatography (see ESI). The half-cell solar-to-hydrogen (HC-STH) conversion efficiency of the Pt/ZnS/CdS-modified photocathode was as high as 1.1% at 0.37 V_{RHE}, while that of the Pt/CdS-modified sample was 0.70% at 0.38 V_{RHE}, as shown in Fig. 10b. The wavelength dependence of the incident-photon-to-current conversion efficiency (IPCE) of the Pt/ZnS/CdS-modified photocathode, as measured at 0 V_{RHE} (Fig. 10c), demonstrates the onset of a cathodic photocurrent in the vicinity of 800 nm. This onset in the IPCE spectrum is in good agreement with the absorption edge of the present $(ZnSe)_{0.85}(CIGS)_{0.15}$ particles, indicating that the PEC hydrogen evolution was triggered by the band gap photoexcitation of the $(ZnSe)_{0.85}(CIGS)_{0.15}$ and that the weak light absorption of this material at longer wavelengths than the absorption edge did not contribute to the PEC reaction. The IPCE became greater than 25% in the shorter wavelength region (below 560 nm) and reached 34% at 360 nm. These PEC characteristics are certainly among the highest values ever observed among this type of particulate photocathode. Therefore, it is apparent that the techniques proposed in this study, including the utilization of Na_2S and improving the electrode surface and backside structure, are viable means of obtaining an efficient Cu-chalcogenide photocathode for sunlight-driven hydrogen production.

Conclusions

The conditions for the synthesis of the particulate solid solution $(ZnSe)_{0.85}(CIGS)_{0.15}$ were carefully investigated while using various amounts of a Cu precursor to generate Cu-deficient, stoichiometric, and Cu-excess materials. A Na_2S additive was also employed to improve the PEC performance. All solid solutions showed an obvious cathodic photoresponse due to incorporation of Li from the flux and the suppression of Zn anti-sites. The Na_2S also promoted the insertion of Li and O into the solid solution and thus more than doubled the cathodic photocurrent. The optimal photocathode was made from stoichiometric $(ZnSe)_{0.85}(CuIn_{0.7}Ga_{0.3}Se_2)_{0.15}$ particles synthesized with Na_2S in conjunction with an appropriate electrode structure, Pt/ZnS/CdS surface modification, and a Mo/C back contact. This device demonstrated an onset potential as high as 0.77 V_{RHE}, a -5.2 mA cm^{-2} photocurrent at 0 V_{RHE} and a 1.1% HC-STH at 0.37 V_{RHE}. These are among the highest values yet reported for a particulate photocathode, and so the present study suggests a new approach to preparing particulate Cu-chalcogenide photocathodes for efficient sunlight-driven hydrogen evolution.

Conflicts of interest

There are no conflicts to declare.

Acknowledgements

This work was supported by the Precursory Research for Embryonic Science and Technology (PRESTO) project (no. JPMJPR1543) of the Japan Science and Technology Agency (JST). Y.K. is a Research Fellow of the Japan Society for the Promotion of Science (JSPS) and acknowledges the support of the JSPS through a Grant-in-Aid for JSPS Fellows (No. 16J04338). This work was also funded in part by Grants-in-Aid for Scientific Research (A) (Nos. 16H02417 and 17H01216) from the JSPS.

References

1. (a) T. Hisatomi, J. Kubota and K. Domen, *Chem Soc Rev*, 2014, **43**, 7520-7535; (b) J. W. Ager, M. R. Shaner, K. A. Walczak, I. D. Sharp and S. Ardo, *Energy & Environmental Science*, 2015, **8**, 2811-2824; (c) K. Takanabe, *ACS Catalysis*, 2017, **7**, 8006-8022.
2. A. Ebina, E. Fukunaga and T. Takahashi, *Physical Review B*, 1974, **10**, 2495-2500.
3. R. N. Noufi, P. A. Kohl and A. J. Bard, *Journal of The Electrochemical Society*, 1978, **125**, 375-379
4. A. Kudo and Y. Miseki, *Chem Soc Rev*, 2009, **38**, 253-278.
5. (a) T. Wada, S. Nakamura and T. Maeda, *Progress in Photovoltaics: Research and Applications*, 2012, **20**, 520-525; (b) M. Moriya, T. Minegishi, H. Kumagai, M. Katayama, J. Kubota and K. Domen, *J Am Chem Soc*, 2013, **135**, 3733-3735; (c) H. Kumagai, T. Minegishi, N. Sato, T. Yamada, J. Kubota and K. Domen, *Journal of Materials Chemistry A*, 2015, **3**, 8300-8307; (d) H. Kaneko, T. Minegishi and K. Domen, *Coatings*, 2015, **5**, 293-311; (e) J. Luo, Z. Li, S. Nishiwaki, M. Schreier, M. T. Mayer, P. Cendula, Y. H. Lee, K. Fu, A. Cao, M. K. Nazeeruddin, Y. E. Romanyuk, S. Buecheler, S. D. Tilley, L. H. Wong, A. N. Tiwari and M. Grätzel, *Advanced Energy Materials*, 2015, **5**; (f) W. Septina, Gunawan, S. Ikeda, T. Harada, M. Higashi,

R. Abe and M. Matsumura, *The Journal of Physical Chemistry C*, 2015, **119**, 8576-8583; (g) Gunawan, W. Septina, T. Harada, Y. Nose and S. Ikeda, *ACS Appl Mater Interfaces*, 2015, **7**, 16086-16092; (h) L. Zhang, T. Minegishi, M. Nakabayashi, Y. Suzuki, K. Seki, N. Shibata, J. Kubota and K. Domen, *Chemical Science*, 2015, **6**, 894-901; (i) N. Guijarro, M. S. Prévot, X. Yu, X. A. Jeanbourquin, P. Bornoz, W. Bourée, M. Johnson, F. Le Formal and K. Sivula, *Advanced Energy Materials*, 2016, **6**.

6. (a) H. Kaneko, T. Minegishi, M. Nakabayashi, N. Shibata, Y. Kuang, T. Yamada and K. Domen, *Advanced Functional Materials*, 2016, **26**, 4570-4577; (b) H. Kaneko, T. Minegishi, M. Nakabayashi, N. Shibata and K. Domen, *Angew Chem Int Ed Engl*, 2016, **55**, 15329-15333.
7. Y. Kuang, Q. Jia, H. Nishiyama, T. Yamada, A. Kudo and K. Domen, *Advanced Energy Materials*, 2016, **6**.
8. T. Higashi, H. Kaneko, T. Minegishi, H. Kobayashi, M. Zhong, Y. Kuang, T. Hisatomi, M. Katayama, T. Takata, H. Nishiyama, T. Yamada and K. Domen, *Chem Commun (Camb)*, 2017, **53**, 11674-11677.
9. J. L. Shay, B. Tell, H. M. Kasper and L. M. Schiavone, *Physical Review B*, 1972, **5**, 5003-5005.
10. Y. Goto, T. Minegishi, Y. Kageshima, T. Higashi, H. Kaneko, Y. Kuang, M. Nakabayashi, N. Shibata, H. Ishihara, T. Hayashi, A. Kudo, T. Yamada and K. Domen, *J. Mater. Chem. A*, 2017, **5**, 21242-21248.
11. (a) Q. Wang, Y. Li, T. Hisatomi, M. Nakabayashi, N. Shibata, J. Kubota and K. Domen, *Journal of Catalysis*, 2015, **328**, 308-315; (b) Q. Wang, T. Hisatomi, Q. Jia, H. Tokudome, M. Zhong, C. Wang, Z. Pan, T. Takata, M. Nakabayashi, N. Shibata, Y. Li, I. D. Sharp, A. Kudo, T. Yamada and K. Domen, *Nat Mater*, 2016, **15**, 611-615; (c) Q. Wang, T. Hisatomi, Y. Suzuki, Z. Pan, J. Seo, M. Katayama, T. Minegishi, H. Nishiyama, T. Takata, K. Seki, A. Kudo, T. Yamada and K. Domen, *J Am Chem Soc*, 2017, **139**, 1675-1683; (d) S. Sun, T. Hisatomi, Q. Wang, S. Chen, G. Ma, J. Liu, S. Nandy, T. Minegishi, M. Katayama and K. Domen, *ACS Catalysis*, 2018, DOI: 10.1021/acscatal.7b03884, 1690-1696.
12. (a) T. Nakada, D. Iga, H. Ohbo and A. Kunioka, *Japanese Journal of Applied Physics*, 1997, **36**, 732-737; (b) M. Kemell, M. Ritala and M. Leskelä, *Critical Reviews in Solid State and Materials Sciences*, 2005, **30**, 1-31.
13. (a) T. Minegishi, N. Nishimura, J. Kubota and K. Domen, *Chemical Science*, 2013, **4**; (b) Y. Ham, T. Minegishi, T. Hisatomi and K. Domen, *Chem Commun*, 2016, **52**, 5011-5014.
14. (a) S.-H. Han, A. M. Hermann, F. S. Hasoon, H. A. Al-Thani and D. H. Levi, *Applied Physics Letters*, 2004, **85**, 576-578; (b) S.-H. Han, F. S. Hasoon, H. A. Al-Thani, A. M. Hermann and D. H. Levi, *Journal of Physics and Chemistry of Solids*, 2005, **66**, 1895-1898.
15. C. Guillén and J. Herrero, *physica status solidi (a)*, 2006, **203**, 2438-2443.
16. (a) M. Miyauchi, M. Takashio and H. Tobimatsu, *Langmuir*, 2004, **20**, 232-236; (b) B. Siritanaratkul, K. Maeda, T. Hisatomi and K. Domen, *ChemSusChem*, 2011, **4**, 74-78; (c) K. Maeda, M. Higashi, B. Siritanaratkul, R. Abe and K. Domen, *J Am Chem Soc*, 2011, **133**, 12334-12337; (d) T. Hisatomi, C. Katayama, Y. Moriya, T. Minegishi, M. Katayama, H. Nishiyama, T. Yamada and K. Domen, *Energy & Environmental Science*, 2013, **6**.
17. R. D. Shannon, *Acta Crystallographica Section A*, 1976, **32**, 751-767.
18. L. Kronik, D. Cahen and H. W. Schock, *Adv Mater*, 1998, **10**, 31-36.
19. (a) T. Wada, N. Kohara, T. Negami and M. Nishitani, *Japanese Journal of Applied Physics*, 1996, **35**, L1253-L1256; (b) N. Kohara, S. Nishiwaki, Y. Hashimoto, T. Negami and T. Wada, *Solar Energy Materials and Solar Cells*, 2001, **67**, 209-215.

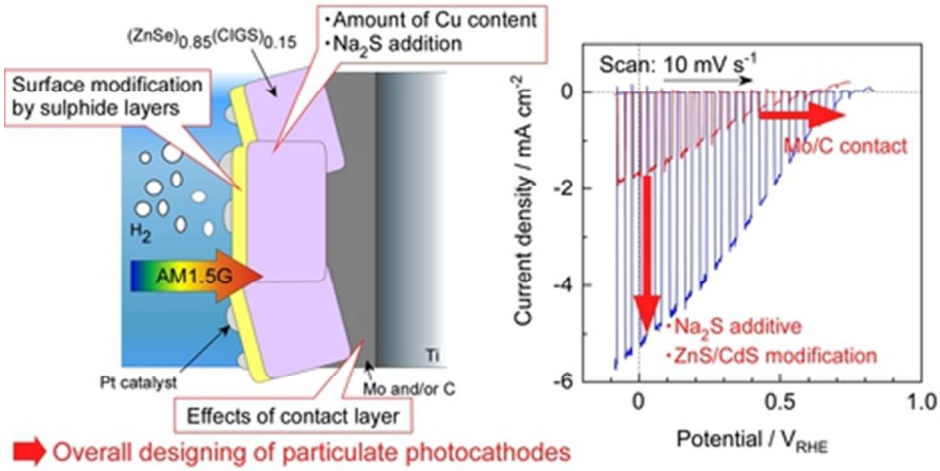

39x20mm (300 x 300 DPI)